Electronic Supplementary Material (ESI) for Journal of Materials Chemistry C.

Supplementary Information

$[C_3N_6H_7]_2[B_3O_3F_4(OH)]$: A new hybrid birefringent crystal with strong optical anisotropy induced by mixed functional units

Congcong Jin[1,2], Fuming Li[1,2], Zhihua Yang[1,2], Shilie Pan[1,2]* and Miriding Mutailipu[1,2]*

[1] CAS Key Laboratory of Functional Materials and Devices for Special Environments, Xinjiang Technical Institute of Physics & Chemistry, CAS, and Xinjiang Key Laboratory of Electronic Information Materials and Devices, 40-1 South Beijing Road, Urumqi 830011, China
[2] Center of Materials Science and Optoelectronics Engineering, University of Chinese Academy of Sciences, Beijing 100049, China
* Corresponding authors: miriding@ms.xjb.ac.cn; slpan@ms.xjb.ac.cn

Experimental section

Reagents and synthesis

Melamine ($C_3N_6H_6$, 98 %), hydrofluoric acid (ω > 40 %), and H_3BO_3 (98 %) were purchased from Shanghai Aladdin Biochemical Technology Co., Ltd. $C_3N_6H_8F_2$ is prepared by the reaction of excessive hydrofluoric acid and melamine. Single crystals of **MelBF** were obtained via mild molten method using boric acid as the flux. $C_3N_6H_8F_2$ and boric acid were mixed homogeneously according to stoichiometric ratio and sealed in a Teflon-lined bomb at 180 °C for 4000 minutes and then slowly cooled to 40 °C with a rate of 1 °C/h. The powder polycrystalline of **MelBF** is easily to get if the calcination temperature of programmed is changed to 160 °C.

Characterization

Single crystal for structure determination of title compound was selected and picked under an optical microscope. The diffraction data for structural refinement were collected on a Bruker D8 Venture with graphite monochromated Mo Ka radiation at room temperature. SAINT and SCALE programs help to complete the integration and absorption corrections.[1] The structures were solved by direct methods and then refined by full-matrix least squares on F^2 with SHELXTL-14 and all non-H atoms were refined anisotropically.[2] Powder X-ray diffraction data were collected on a Bruker D2 Phaser X-ray diffractometer equipped with Cu Ka radiation (λ = 1.54056 Å). Polycrystalline powder of title compound was characterized by solid state nuclear magnetic resonance (NMR), which was carried out with a Bruker Avance III 500 WB (11.75 T) spectrometer. The experimental detail for NMR goes in exactly the same way as our previous work.[3] The Infrared absorption spectra were recorded on the SHIMADZU IRAffinity-1 Fourier transform infrared spectrometer in the range of 400–4000 cm^{-1} with the resolution of 2 cm^{-1}. The UV-vis-NIR diffuse-reflectance spectra were recorded by a SolidSpec-3700DUV spectrophotometer in the range of 180 to 2600 nm with a scan step width of 2 nm at room temperature and nitrogen atmosphere. Thermal properties were characterized by using a NETZSCH STA 449F3 simultaneous analyzer with a heating rate of 5 °C per minute under the nitrogen atmosphere, and the temperature range is 50–800 °C.

Computational description

Theoretical calculations of **MelBF** were done with the plane-wave pseudopotential method implemented in the CASTEP package, and the electronic structures were simulated based on density functional theory (DFT).[4] The optimized norm-conserving pseudopotentials were utilized to simulate ion-electron interactions for all the constituent elements.[5] **MelBF** was optimized by the Perdew-Burke-Ernzerhof (PBE) exchange-correlation of Generalized Gradient Approximation (GGA).[6] The atomic positions in the unit cell were fully optimized using BFGS method. In **MelBF**, the C $2s^22p^2$, N $2s^22p^3$, B $2s^22p^1$, O $2s^22p^4$, H $1s^1$, and F $2s^22p^5$ were treated as the valence electrons. Also, kinetic energy cut-offs were reasonable set (850.0 eV) and Monkhorst-Pack k-point meshes ($4 \times 3 \times 2$) with a density of fewer than 0.04 $Å^{-1}$ in the Brillouin zone (BZ). The empty bands were set as 3 times that of valence bands in the calculation. The other calculation parameters and convergent criteria were the default values of the CASTEP code. Although the GGA-PBE method is adequately eligible to describe the electronic structures and optical properties in terms of numerous crystals.[7] The scissors operation was used here to simulate the electric field of the real condition strictly.

Table S1. Crystal data and structure refinement for **MelBF**.

Formula	$\mathbf{[C_3N_6H_7]_2[B_3O_3F_4(OH)]}$
Formula weight	427.73
Temperature/K	300
Crystal system	Triclinic
Space group	$P\bar{1}$
a/Å	6.9987(4)
b/Å	10.0087(4)
c/Å	11.5314(5)
α/°	90.031(2)
β/°	94.120(2)
γ/°	94.442(2)
Volume/Å^3	803.23(7)
Z	2
$\rho_{calc.}$ / g/cm^3	1.769
μ/mm^{-1}	0.167
F(000)	436.0
Radiation	Mo Kα ($\lambda = 0.71073$)
2θ range/°	3.542 to 50.054
Index ranges	$-8 \leq h \leq 8$, $-11 \leq k \leq 11$, $-13 \leq l \leq 13$
Reflns collected	29258
Unique reflns (R_{int})	2834 ($R_{int} = 0.0717$)
Data/restraints/param	2834/0/305
Goodness-of-fit on F^2	1.071
$R_1$$^{a)}$/$wR_2$$^{b)}$ [$I \geq 2\sigma(I)$]	0.0410/0.1006
$R_1$$^{a)}$/$wR_2$$^{b)}$ [all data]	0.0543/0.1156
Largest diff. peak/hole	0.26/-0.24 (e Å^{-3})

a) $R_1 = \Sigma||F_o|-|F_c||/\Sigma|F_o|$ and b) $wR_2 = [\Sigma w(F_o^2 - F_c^2)^2/\Sigma wF_o^4]^{1/2}$.

Table S2. Fractional atomic coordinates (×10^4) and equivalent isotropic displacement parameters (Å^2×10^3) for all non-H atoma in the asymmetric unit for **MelBF**. U_{eq} is defined as 1/3 of the trace of the orthogonalised U_{ij} tensor.

Atom	*x*	*y*	*z*	U(eq)
C1	8817(3)	2872(2)	9796.4(17)	26.4(5)
C2	7677(3)	909(2)	10565.8(18)	27.4(5)
C3	7951(3)	2920(2)	11648.6(17)	25.9(4)
C4	1788(3)	1259(2)	2662.6(18)	29.2(5)
C5	2043(3)	3117(2)	3786.2(18)	29.4(5)
C6	2953(3)	3197(2)	1867.9(17)	26.6(5)
N1	9577(3)	3520(2)	8925.2(17)	35.5(5)
N2	8314(3)	1550.7(17)	9651.6(15)	29.4(4)
N3	7206(3)	-387.0(19)	10526.4(19)	36.7(5)
N4	7488(3)	1578.0(17)	11585.2(16)	28.8(4)
N5	7723(3)	3532(2)	12639.8(16)	34.7(5)
N6	8633(3)	3602.0(16)	10767.9(14)	27.1(4)
N7	1329(3)	-40.4(19)	2550.5(19)	39.2(5)
N8	1519(3)	1821.0(18)	3688.1(15)	33.8(4)
N9	1777(3)	3767(2)	4747.9(17)	39.6(5)
N10	2819(3)	3826.4(19)	2900.3(15)	29.4(4)
N11	3608(3)	3925(2)	1009.0(17)	34.0(5)
N12	2450(3)	1903.8(17)	1720.8(15)	29.5(4)
B1	4428(4)	914(2)	6475(2)	28.5(5)
B2	4299(4)	3027(2)	7520(2)	27.5(5)
B3	6576(4)	2825(2)	5953(2)	27.9(5)
O1	3778(3)	-408.0(15)	6370.8(13)	38.3(4)
O2	3872(2)	1593.7(14)	7393.8(13)	35.7(4)
O3	5772(2)	3562.8(14)	6831.9(13)	32.1(4)
O4	5591(2)	1508.5(14)	5706.5(12)	30.6(4)
F1	4788(2)	3313.1(13)	8728.0(10)	38.5(3)
F2	2567.8(19)	3663.4(13)	7262.8(11)	41.2(4)
F3	8542.0(19)	2677.1(14)	6273.0(13)	44.2(4)
F4	6544(2)	3554.3(13)	4894.4(11)	40.4(4)

Table S3. The bond valence sum (BVS) for all non-H atoms in $[B_3O_3F_4(OH)]$ unit for **MelBF**. The bond valences for each non-H atom in $[B_3O_3F_4(OH)]$ unit are calculated according to the following equation: bond valence = exp[(R_o-R)/B], where R is the bond length. The bond valence parameter is as follow: R_o(B-O) = 1.371 Å, B(B-O) = 0.37; R_o(B-F) = 1.281 Å, B(B-F) = 0.37; R_o(H-O) = 0.907 Å, and B(H-O) = 0.28.[8]

$[B_3O_3F_4(OH)]$ in $[C_3N_6H_7]_2[B_3O_3F_4(OH)]$ (MelBF)			
B1	3.10	O4	1.84
B2	3.03	F1	0.66
B3	3.03	F2	0.68
O1	1.97	F3	0.69
O2	1.86	F4	0.68
O3	1.74		

Table S4. Selected bond lengths (Å) and angles (deg.) in **MelBF**.

B1-O1	1.367(3)	C2-N3	1.313(3)
B1-O2	1.356(3)	C2-N4	1.372(3)
B1-O4	1.353(3)	C3-N4	1.357(3)
B2-F1	1.434(3)	C3-N5	1.322(3)
B2-F2	1.424(3)	C3-N6	1.321(3)
B2-O2	1.448(3)	C4-N7	1.320(3)
B2-O3	1.418(3)	C4-N8	1.341(3)
B3-F3	1.418(3)	C4-N12	1.355(3)
B3-F4	1.423(3)	C5-N8	1.323(3)
B3-O3	1.427(3)	C5-N9	1.317(3)
B3-O4	1.457(3)	C5-N10	1.365(3)
C1-N1	1.318(3)	C6-N10	1.359(3)
C1-N2	1.349(3)	C6-N11	1.318(3)
C1-N6	1.356(3)	C6-N12	1.322(3)
C2-N2	1.322(3)		
O2-B1-O1	116.73(19)	N2-C2-N4	120.92(18)
O4-B1-O1	121.63(19)	N3-C2-N2	121.06(19)
O4-B1-O2	121.64(19)	N3-C2-N4	118.02(19)
F1-B2-O2	107.83(17)	N5-C3-N4	117.54(19)
F2-B2-F1	104.37(17)	N6-C3-N4	122.08(18)
F2-B2-O2	108.31(18)	N6-C3-N5	120.36(19)
O3-B2-F1	110.73(17)	C2-N2-C1	116.28(17)
O3-B2-F2	110.88(18)	C3-N4-C2	119.31(18)
O3-B2-O2	114.21(18)	C3-N6-C1	115.39(17)
F3-B3-F4	105.69(18)	N7-C4-N8	117.0(2)
F3-B3-O3	109.66(18)	N7-C4-N12	116.79(19)
F3-B3-O4	109.22(18)	N8-C4-N12	126.23(19)
F4-B3-O3	110.16(18)	N8-C5-N10	121.87(19)
F4-B3-O4	107.53(17)	N9-C5-N8	120.0(2)
O3-B3-O4	114.21(18)	N9-C5-N10	118.1(2)
B1-O2-B2	121.38(17)	N11-C6-N10	117.44(19)
B2-O3-B3	123.97(16)	N11-C6-N12	120.77(19)
B1-O4-B3	120.70(17)	N12-C6-N10	121.79(19)
N1-C1-N2	117.63(19)	C5-N8-C4	115.58(18)
N1-C1-N6	116.45(18)	C6-N10-C5	118.82(18)
N2-C1-N6	125.92(18)	C6-N12-C4	115.52(17)

Table S5. Hydrogen bonds in **MelBF**.

D-H···A	d(D-A)/Å	D-H···A/°
O1-H1···O4^{1}	2.715(2)	177.6
N1-H2···N6^{2}	3.061(3)	177(2)
N3-H4···N12^{3}	3.036(3)	177(2)
N3-H5···O2^{4}	2.811(3)	177(3)
N4-H6···O1^{4}	2.803(2)	175(2)
N5-H7···F4^{5}	2.784(2)	136(2)
N5-H8···F2^{6}	2.832(2)	164(2)
N7-H9···N2^{3}	2.990(3)	175(2)
N7-H10···F3^{3}	2.973(2)	128(2)
N9-H11···F2^{7}	2.916(2)	123(2)
N9-H11···F3^{5}	3.098(3)	146(2)
N9-H12···F4^{2}	2.860(2)	178(2)
N10-H13···O3^{2}	2.730(2)	177(2)
N11-H14···F1^{8}	2.909(2)	174(2)
N11-H15···F1^{8}	2.892(2)	155(2)

Symmetry codes:

^{1} $1-x,-y,1-z$; ^{2} $2-x,1-y,2-z$; ^{3} $2-x,-y,2-z$;
^{4} $1-x,-y,2-z$; ^{5} $1+x,+y,+z$; ^{6} $1-x,1-y,2-z$;
^{7} $1+x,+y,1+z$; ^{8} $1+x,+y,+z$.

Table S6. Assignment of the absorption peaks observed in the IR spectrum for **MelBF**.

Mode description	Absorption peaks (cm^{-1})
$\upsilon_{as}(NH_2)$, $\upsilon_s(NH_2)$	3360, 3252
$\upsilon(OH)$	3448
$\upsilon(NH\cdots N)$	3144
$\upsilon(NH\cdots O)$	2916
$\sigma(NH_2)$	1674, 1662
υ_{as}(side-chain C-N)	1558, 1508
$\tau(NH_2)$	482
$\upsilon_{as}(BO_3)$, $\upsilon_s(BO_3)$	1420, 949
$\tau(BO_3$, out of plane)	760, 721
$\tau(BO_3)$	536
υ_{as}(B-F)	1362
υ_s(B-F, out of phase)	806

Figure S1. The asymmetric unit for **MelBF** and the dihedral angle between [$B_3O_3F_4(OH)$] and [$C_3N_6H_7$] units.

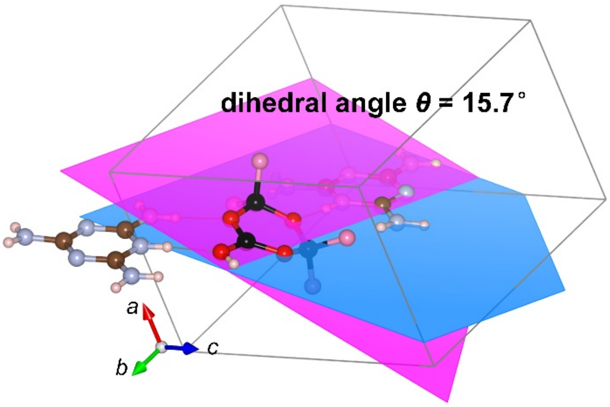

Figure S2. Experimental and calculated XRD patterns for **MelBF**.

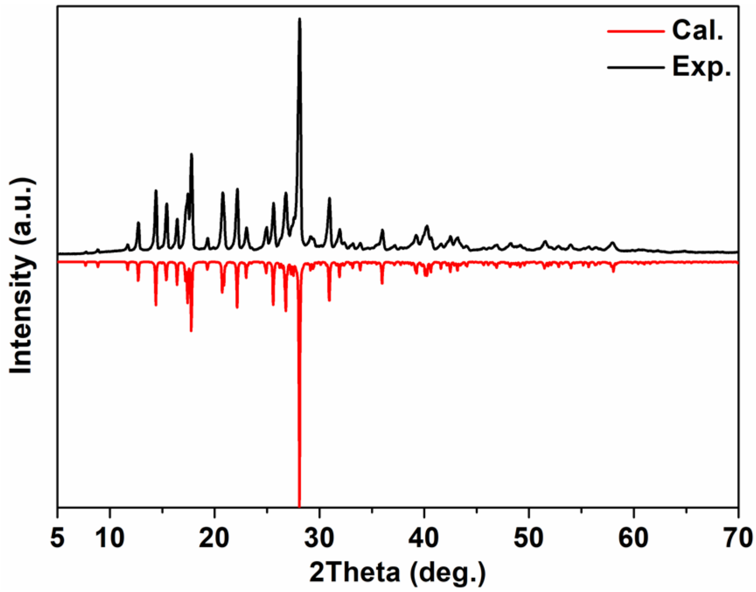

Figure S3. Temperature-dependent XRD data collected in the range of 120-300 °C for **MelBF**.

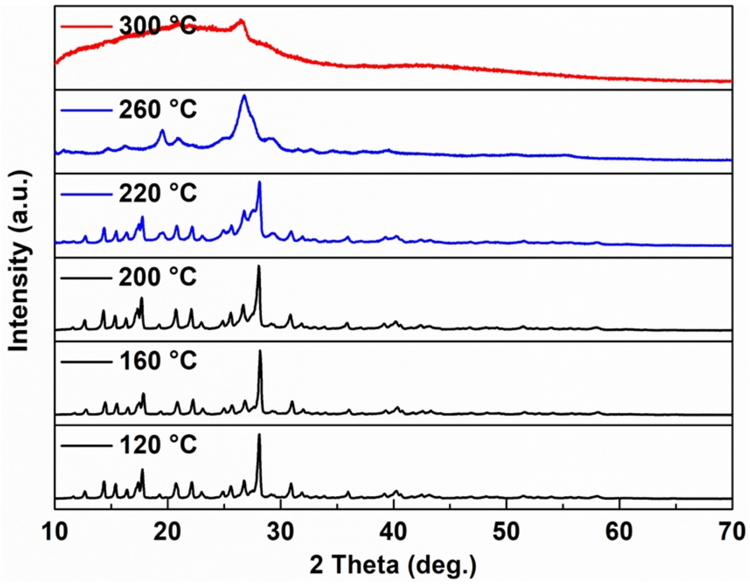

Figure S4. Optical absorption spectrum for **MelBF**.

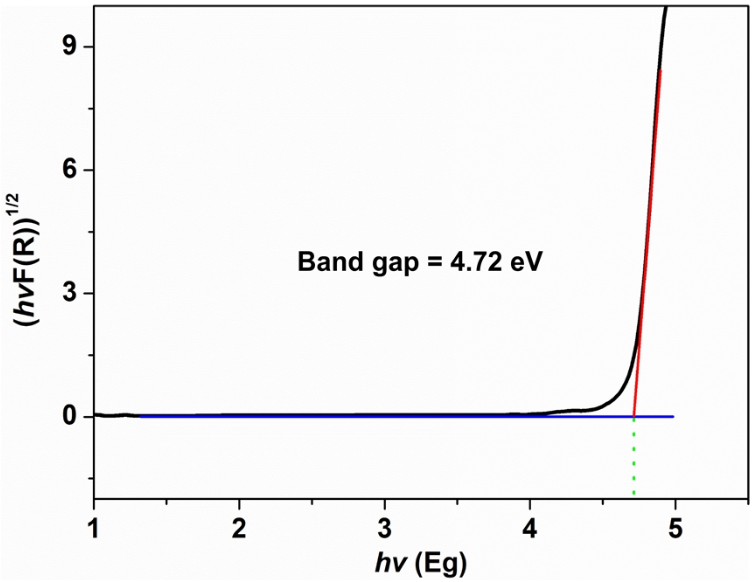

References

1 SAINT Plus, Version 7.60A; Bruker Analytical X-ray Instruments, 2000.

2 G. M. Sheldrick, *Acta Crystallogr. C*, 2015, **71**, 3.

3 (a) C. C. Jin, X. P. Shi, H. Zeng, S. J. Han, Z. Chen, Z. H. Yang, M. Mutailipu and S. L. Pan, *Angew. Chem., Int. Ed.*, 2021, **60**, 20469; (b) C. C. Jin, H. Zeng, F. Zhang, H. T. Qiu, Z. H. Yang, M. Mutailipu and S. L. Pan, *Chem. Mater.*, 2022, **34**, 440.

4 (a) M. Segall, P. Lindan, M. J. Probert, C. J. Pickard, P. J. Hasnip, S. J. Clark and M. C. Payne, *J. Phys. Condens. Mater.*, 2002, **14**, 2717; (b) S. J. Clark, M. D. Segall, C. J. Pickard, P. J. Hasnip, M. J. Probert, K. Refson and M. C. Payne, *Z Kristallogr*, 2005, **220**, 567; (c) T. Gilbert, *Phys. Rev. B*, 1975, **12**.

5 J. S. Lin, A. Qteish, M. C. Payne and V. Heine, *Phys. Rev. B*, 1993, **47**, 4174.

6 (a) M. Fuchs and M. Scheffler, *Comput. Phys. Commun.*, 1999, **119**, 67; (b) J. P. Perdew, J. A. Chevary, S. H. Vosko, K. A. Jackson, M. R. Pederson, D. J. Singh and C. Fiolhais, *Phys. Rev. B*, 1992, **46**, 6671.

7 H. Englisch and R. Englisch, *Phys. A*, 1983, **121**, 253.

8 I. D. Brown, D. Altermatt, *Acta Crystallogr.*, *Sect B-Struct. Sci.*, 1985, **41**, 244.